Polymer Vol. 39 No. 23, pp. 5725–5730, 1998
0032-3861/98/$ – see front matter

PII: S0032-3861(97)10344-5

An atomic force microscopy study of the molecular organisation of xanthan

I. Capron, S. Alexandre and G. Muller*
UMR CNRS 6522, Polymères, Biopolymères et Membranes, Université de Rouen, 76821 Mont-Saint-Aignan, Cedex, France
(Accepted 18 November 1997)

Xanthan molecules derived from dilute and semi-dilute solutions which have been heated above the order–disorder melting temperature T_m and thereafter cooled below T_m were imaged by atomic force microscopy (AFM). A new method which avoids the drying step of the sample has been used to give images of individual xanthan molecules. It has also been possible to obtain images of aggregated molecules organised in a network structure. Such an organisation agrees with the otherwise observed dependence of the rheological behaviour on the thermal treatment. © 1998 Elsevier Science Ltd. All rights reserved.

(Keywords: atomic force microscopy; xanthan; conformation)

INTRODUCTION

Xanthan is an anionic exopolysaccharide mainly used as a thickening or stabilising agent in a variety of applications. Its well-known and remarkable rheological properties come mainly from a high molecular weight associated with a helical structure making xanthan a semi-rigid rod-like molecule[1–7].

Many experimental evidences suggest that native xanthan exists as a double-stranded structure which can be partially or totally dissociated into single stranded flexible molecules upon heating above a salt-dependent critical temperature T_m[8–11]. On renaturation by cooling below T_m the reassembly of chains generates an architecture which differs from the original one and depends on whether the heat treatment was performed on dilute or concentrated solution, in the presence or absence of salt. At high polymer concentration and ionic strength, an intermolecular ordering or self-aggregation through hydrogen bonding, entanglement effects and/or apolar associations can become increasingly significant[13]. These non-covalent intermolecular interactions can confer 'weak-gel' properties to xanthan.

Recently we have shown that the solution properties and more specifically the macroscopic rheological behaviour of the xanthan molecule are related to the thermal history the sample has been subjected to[12]. The difference between the solution properties of xanthan before (native ordered form) and after (renatured form) heat treatment above T_m can be explained by the fact that the biopolymer assumes different molecular architectures.

A number of papers report that electron microscopies are interesting techniques to investigate the molecular architecture of polysaccharides[14–18]. Scanning tunnelling microscopy (STM) can image biological molecules deposited onto conducting substrates, but the resolution can be restricted by the grain size of the coating. At first, most efforts have been concentrated upon the imaging of DNA and proteins. Then the technique has been applied to carbohydrates and recent studies have been reported which concern various polysaccharides such as amylose, carrageenans and several cellulose derivatives including xanthan[14–18]. Wilkins *et al.*[16] notably emphasized a number of difficulties encountered when imaging this kind of biopolymer e.g. image penetration, the presence of substrate features and the lack of reproducibility. These authors claim that spray deposition followed by metal coating is the most reliable process although the resolution is limited.

The atomic force microscopy (AFM) developed in 1986 offers advantages over the use of STM such as the absence of coating (no necessity of conducting materials) and a wider choice of substrates. The first work on xanthan conducted by Meyer *et al.*[19] reported a preliminary study of the molecules adsorbed onto mica showing continuous periodic arrays with no visible individual molecules. Then Kirby *et al.*[20] reported a method to give reproducible images: drops of 20 ppm solution diluted in distilled water were deposited onto mica, air dried, and then imaged under butanol. Under ambient conditions (relative humidity $> 30\%$), a thin layer of water condenses on the surface of the sample and the tip. This gives rise to a capillary force which rams the AFM tip onto the surface with a force typically many times larger than the maximum force acceptable without damage to the molecules. Imaging under alcohol presents a double interest: as alcohol is a precipitant for xanthan, the desorption from the mica surface is limited and the adhesion effect (still not fully understood) of the water–mica system is minimised. Kirby *et al.*[20] observed associated molecules as an array with visible polymer ends and defects.

In this study, we propose a sample preparation that allows the visualisation of the individual molecules. The technique has been applied to analyze the reorganisation of xanthan molecules after heat treatment above T_m.

MATERIALS AND METHODS

The AFM used for this study is a Nanoscope II model from Digital Instrument (Santa Barbara, CA, USA). All the measurements were performed in a 'liquid cell' with the feed-back loop on. The samples were scanned at constant operating force in the range 10^{-9} to 10^{-8} N with a cantilever

* To whom correspondence should be addressed

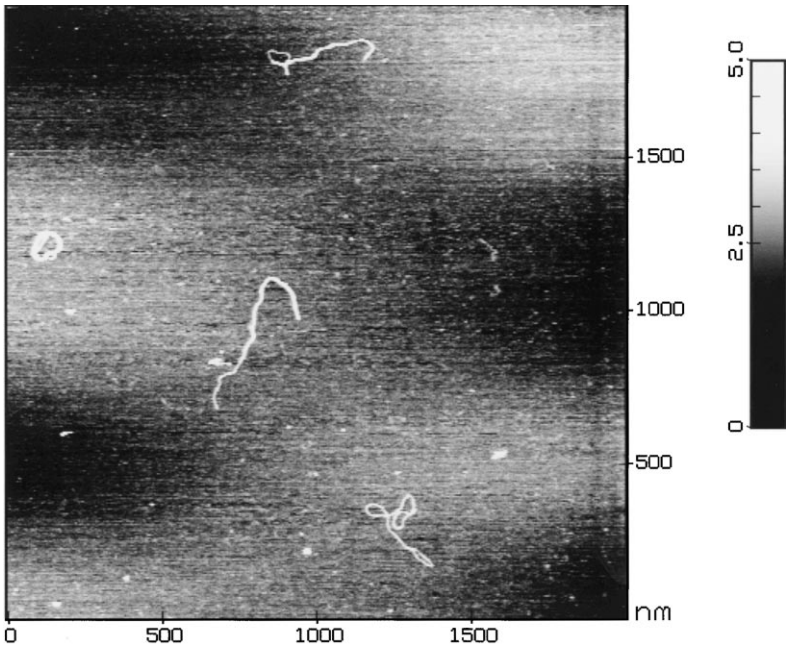

Figure 1 AFM image of native xanthan molecules in water obtained in a liquid cell under isopropanol ($c = 0.2$ mg/L)

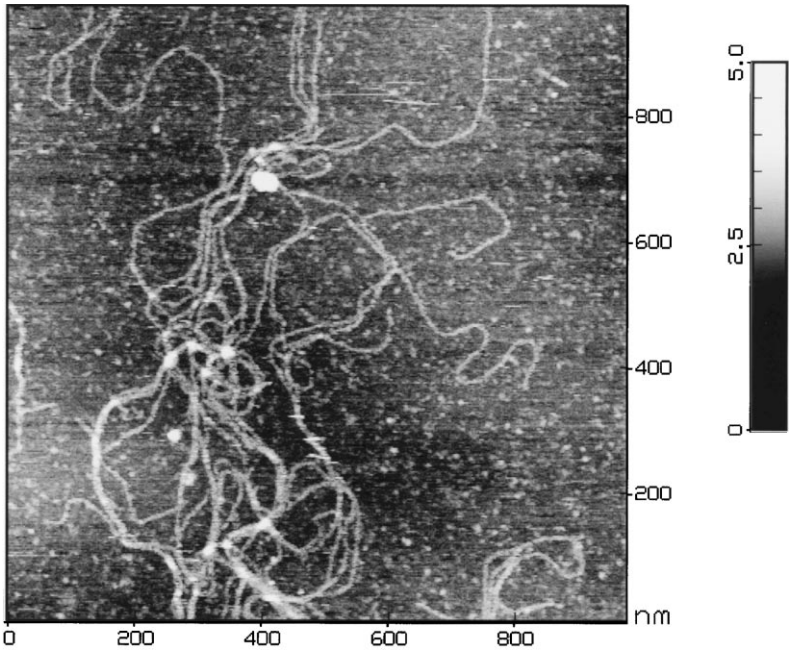

Figure 2 AFM image of native xanthan molecules in 0.01 M NaCl obtained in a liquid cell under isopropanol ($c = 0.2$ mg/L)

characterized by a spring constant of about 0.06 N/m. A 15 μm scanner was used for all visualisations except for the native sample in 0.01 M NaCl which was observed with a 1 μm scanner. The same tip was used for all the images presented here. This allows a good comparison between the various samples avoiding artefacts that could be due to the shape of the tip.

No other processing except for a flattening operation was used in order to obtain the horizontality of the background surface. All images are presented in height mode (palette of grey for height: dark grey for low zones, light grey for high zones).

The commercial xanthan sample was supplied by Systems-Bio-Industries (CX12 lot 41752PO) as a powder, the characteristics of which are reported elsewhere[11] ($M_w = 5.3 \times 10^6$ g/mol, $[\eta] = 7.1$ L/g and $DS_{\text{pyruvate}} = 0.5$). The powder was dispersed in water, gently stirred and kept in a fridge over night. The concentration was then adjusted to 1 g/L for dilute solutions and 20 g/L for concentrated ones by adding water and when necessary 0.01 M NaCl.

The sample preparation consisted of a polymer dilution to 0.2 mg/L with water or with 0.01 M NaCl and a clarification by filtration through 0.22 μ Millipore filters. The solution was then directly injected in the cell, and kept for around one minute to allow the adsorption on a freshly cleaved mica surface. The aqueous solution was then expelled from the AFM cell and immediately replaced with isopropanol.

This new process offers two main advantages: 1) the very low concentration used makes possible the observation of isolated molecules in solution and 2) due to the suppression of the drying step, there is no forced adsorption onto the

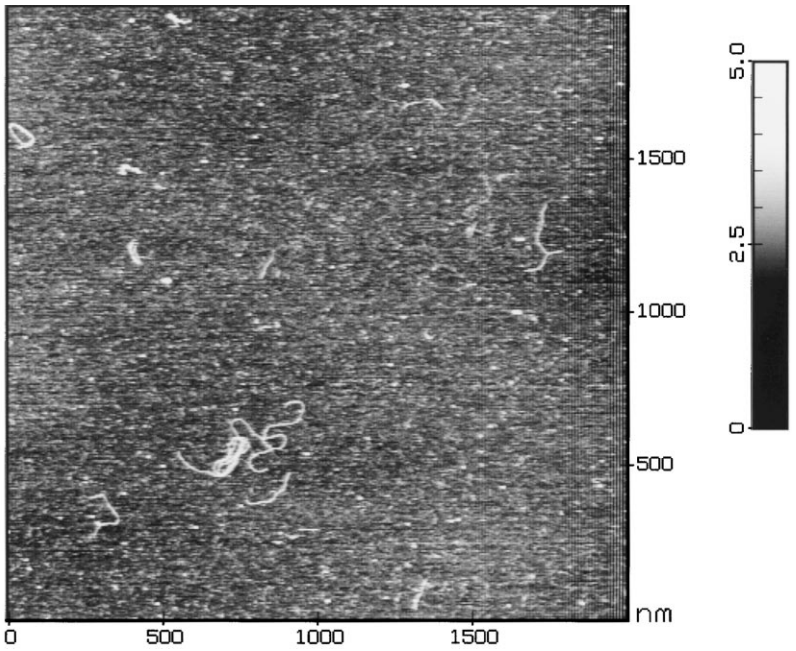

Figure 3 AFM image of renatured xanthan molecules (heated 30 minutes at 90°C) in 0.01 M NaCl, obtained in a liquid cell under isopropanol ($c = 0.2$ mg/L)

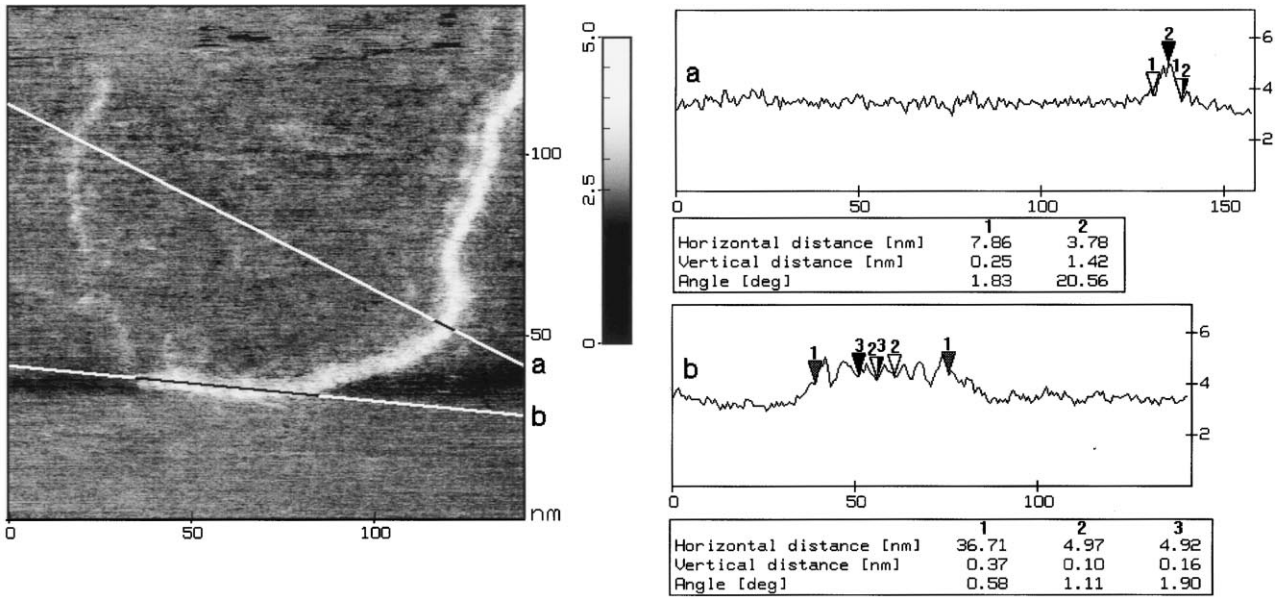

Figure 4 AFM image of xanthan molecules heated 30 minutes at 90°C at 1 g/L in 0.01 M NaCl, obtained in a liquid cell under isopropanol ($c = 0.2$ mg/L). (a) cross section; (b) longitudinal section

surface. The injection of isopropanol allows, in these conditions, a fixation of the molecules while limiting the artefacts induced by the preparation process.

RESULTS

Firstly, the molecules were imaged before and after a thermal treatment performed in a range of concentrations where a dissociation of the double strand occurs as suggested by the halving in molecular weight measured by light scattering[11]. The 1 g/L xanthan solution diluted to 0.2 mg/L in distilled water presents very little adsorption onto the mica and isolated molecules are observed (*Figure 1*). This seems to indicate that the entanglements visualised by Kirby *et al.*[20] might be due to the drying step that can induce a forced adsorption onto the substrate. This method seems more accurate to visualise in a representative way the interactions existing in solution. The molecules observed are around 0.8 μm long, a dimension in accordance with that reported by Stokke *et al.*[21] from electron microscopy observation.

As a comparison, a 1 g/L solution diluted to 0.2 mg/L in 0.01 M NaCl presents many more molecules adsorbed onto the mica surface (*Figure 2*). This agrees with the salt-induced aggregation process reported by several authors[10,22,23]. The presence of knots indicates favourable loci where the intermolecular associations can occur, that could be attributed to highly pyruvated areas and/or the presence of contaminants as apolar zones. They are responsible for the larger molecular weight measured in

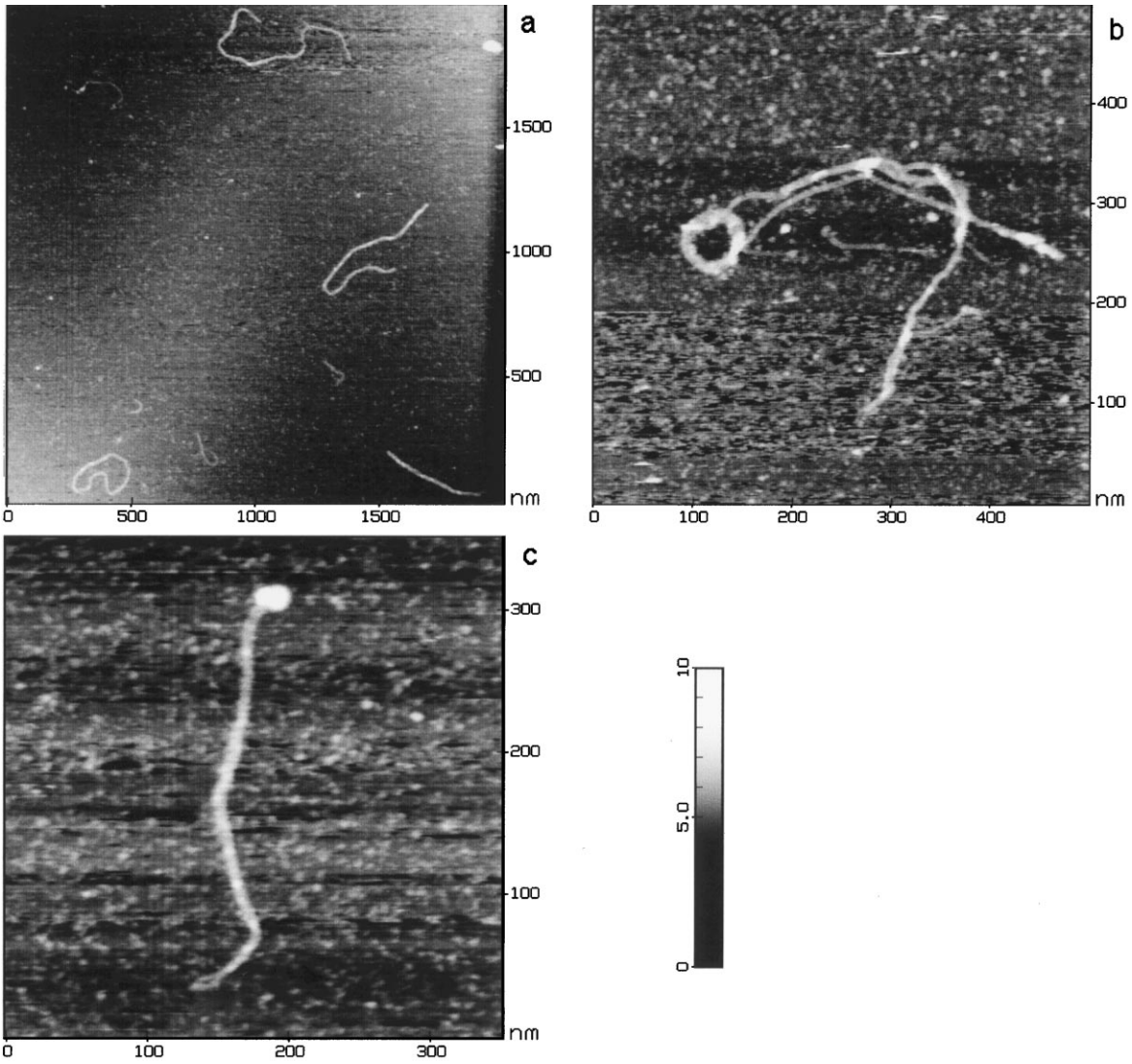

Figure 5 (a), (b) and (c). AFM images of xanthan molecules heated 30 minutes at 90°C at 20 g/L in 0.03 M NaCl, obtained in a liquid cell under isopropanol ($c = 0.2$ mg/L)

the presence of salt. At this concentration (0.2 mg/L) these associations most likely exist in solution, the strong adsorption being attributed to the aggregated structure.

This sample was finally heated for 30 minutes at 90°C in 0.01 M NaCl, and then recorded to 25°C. As well documented this heating/cooling treatment induces an order/disorder/reorder cycle. The same procedure as above was used for visualising the renatured state of xanthan. The image shown in *Figure 3* represents isolated molecules with no visible knots. As the experimental conditions were identical with those used for *Figure 2* this indicates that the aggregated structures previously observed are independent of the substrate–solvent interactions, therefore confirming the salt-induced associations present in a unheated solution. Also we can conclude that during thermal treatment in dilute solution these intermolecular associations can be destroyed. This irreversible disaggregative process has been evidenced using light scattering and viscometry measurements[11]. We may assume that during the thermal treatment, denaturation of proteins occurs and contaminants could be released from the biopolymer, limiting apolar concentration zones. Another possibility (not incompatible with the previous one) is to consider that in this domain of concentration after the dissociation, apolar associations are preferentially

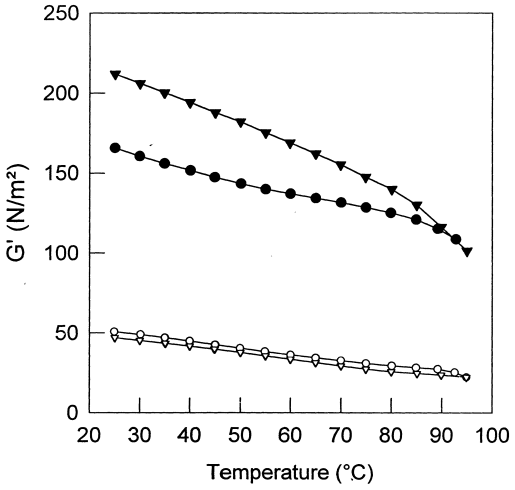

Figure 6 Temperature dependence of the storage modulus G' of native xanthan at 10 g/L (open symbols) and 20 g/L (solid symbols) on heating (circles) and cooling (triangles)

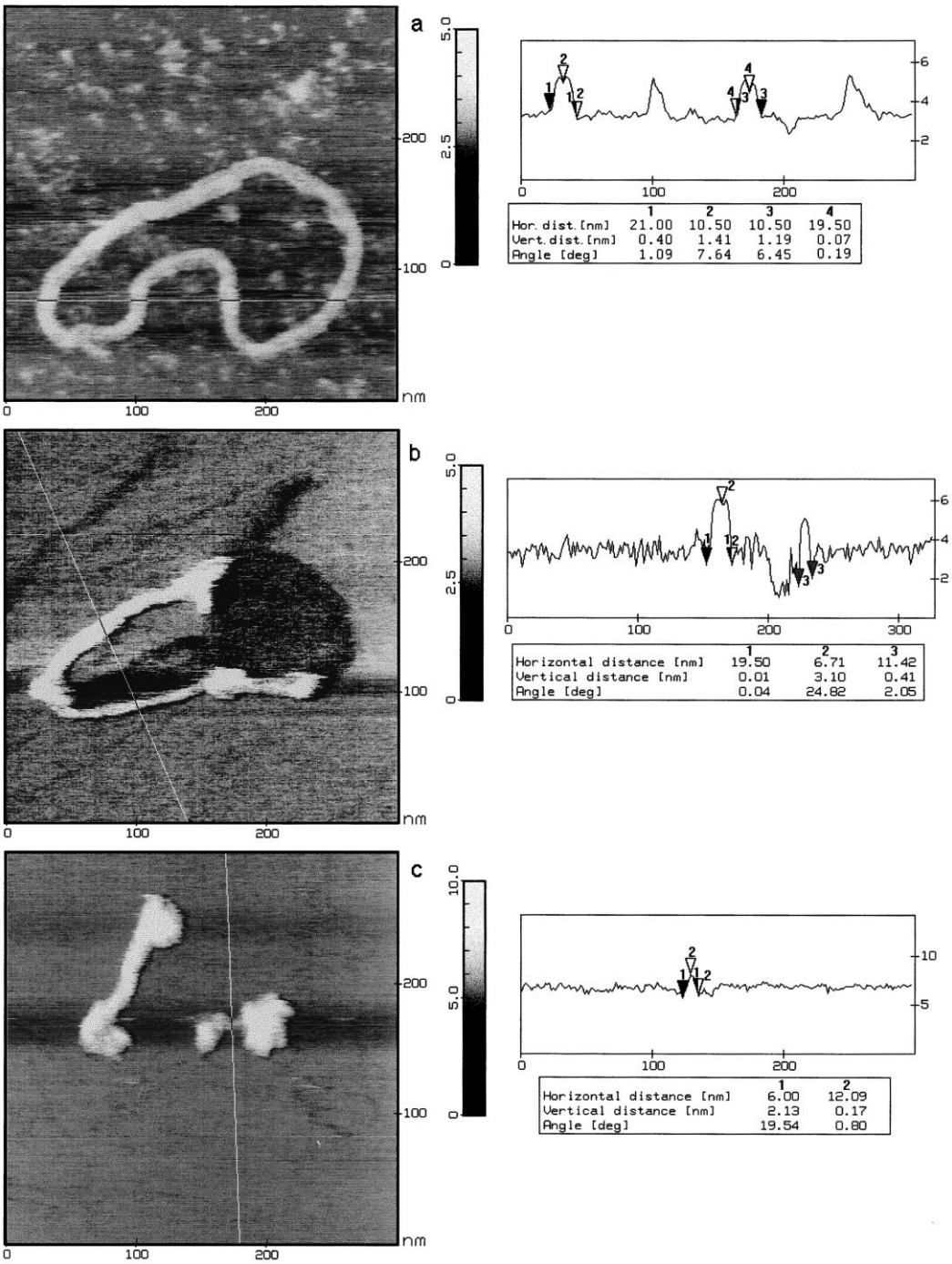

Figure 7 AFM images of xanthan molecules heated 30 minutes at 90°C at 20 g/L in 0.03 M NaCl, obtained in a liquid cell under isopropanol ($c = 0.2$ mg/L). From top to bottom is shown the time dependence of scraping of the surface

intramolecular. Particular organisations of isolated molecules with bifurcations (Y form) that did not appear in native solution were observed. This indicates that the renatured state differs from the native state. After dissociation, imperfect reassociations of single strands result in new duplex structures.

A diameter of around 2 to 4 nm[24] has been reported for the ordered form of the molecule. *Figure 4* shows a representative profile observed for the renatured sample. The molecules imaged are 2 nm in width and 8 nm thick (*Figure 4a*), against 10 nm for the native molecule in 0.01 M NaCl (*Figure 2*). The dimensions, although overestimated due to a probe broadening of the tip extremity, agree rather well with the values expected for an isolated xanthan molecule. This decrease in dimension can be attributed to the suppression of intermolecular links during the denaturation process, implying the dissociation of the double strands. Whereas the width of an isolated molecule is difficult to measure, a helical path can be evaluated with good precision. A helical pitch of 4.9 nm has been measured (*Figure 4b*), whereas X-ray and modelling measurements gave 4.7 nm[24,25]. This value was observed for both native aqueous and renatured salted solutions. It suggests that whatever the native or renatured form, the helical structure is quite identical. This is in accordance with circular dichroism results showing an absence of hysteresis before and after thermal treatment, implying the same global conformational organisation[26].

To show the effect of thermal treatment on semi-dilute and concentrated xanthan solutions, a 20 g/L solution in

0.03 M NaCl was heated to 90°C for 30 minutes and then diluted to 0.2 mg/L in 0.01 M NaCl. We observed little adsorption onto the substrate as was reported for the renatured sample in the dilute concentration range. This is consistent with the disruption of apolar association upon heating. Nevertheless, the renatured molecules appear different from those in dilute solution. Molecules with many intermolecular associations are observed (*Figure 5*). It is interesting to correlate these observations with the variation of the storage modulus G' during the heating/cooling treatment of xanthan. *Figure 6* shows that the change in the storage modulus G' on heating to 95°C and then cooling to 25°C xanthan solutions at concentrations of 10 g/L and 20 g/L respectively can be attributed to the formation of a more structured assembly in the case of the more concentrated solution, contrary to what happens with the lower concentration. Such rheological properties agree with the AFM pictures. Lateral and end-to-end associations (*Figure 5c*) and also loops (bottom of the picture) can be visualized in renatured molecules. This indicates that the chain could fold into a hair-pin type reorganisation.

Several circular loops were also observed. One of them has been studied more precisely and its evolution during scanning has been followed (*Figure 7*). These loops could consist of several associated chains. This assembly could be destroyed as a consequence of scraping of the surface by the tip. The observation of such structures confirms that aggregated structures could be induced by thermal treatment of concentrated xanthan and agrees with the observed viscosity of the renatured xanthan.

Due to the high concentration, the denatured molecules are only partially dissociated because of steric effects. The side chains, aligned along the backbone when the molecule is in an ordered helical form, only partially release from the main chain. In that case dissociation could not occur. The double strands can then form associations with neighbouring molecules; these interactions are maintained when the renaturation conditions are restored. On the other hand, in the dilute solution, the spreading of the side chains interacting with the backbone was followed by an irreversible dissociation of the dimerized molecule into two single chains. This is followed by a folding intramolecular process showing bifurcations but no intermolecular organisations.

This can explain the not yet well understood viscosity increase observed in some cases during thermal treatment, notably during a post-fermentation process as has been reported in a preceding paper[12].

CONCLUSION

Some authors have reported AFM studies showing that reliable images of polysaccharides including xanthan could be obtained using this microscopy technique[20]. This work proposes a more satisfying process compared to the conventional drop deposition method. In the present method the drying step responsible for a superadsorption of the molecules onto the mica surface is avoided. Under appropriate conditions AFM is revealed to be appropriate to obtain a characterization of polymers. Using this technique it has been possible to visualize different molecular architectures of the xanthan molecule which can explain the rheological observations.

REFERENCES

1. Holthwart, G., *Biochemistry*, 1976, **15**, 4333.
2. Morris, E. R., Rees, D. A., Young, G., Walkinshaw, M. D. and Darke, A., *J. Mol. Biol.*, 1977, **110**, 1.
3. Norton, I. T., Goodall, D. M., Frangou, S. A., Morris, E. R. and Rees, D. A., *J. Mol. Biol.*, 1984, **175**, 371.
4. Muller, G., Anrhourrache, M., Lecourtier, J. and Chauveteau, G., *Int. J. Biol. Macromol.*, 1986, **8**, 167.
5. Milas, M. and Rinaudo, M., *Carbohydr. Res.*, 1986, **158**, 191.
6. Liu, W., Sato, T., Norisuye, T. and Fugita, H., *Carbohydr. Res.*, 1987, **160**, 267.
7. Haache, L. S., Washington, G. E. and Brant, D. A., *Macromolecules*, 1987, **20**, 2179.
8. Muller, G. and Lecourtier, J., *Carbohydr. Polym.*, 1988, **9**, 213.
9. Gamini, A. and Mandel, M., *Biopolymers*, 1994, **34**, 783.
10. Kawakami, K., Okabe, Y. and Norisuye, T., *Carbohydr. Polym.*, 1991, **14**, 189.
11. Capron, I., Brigand, G. and Muller, G., *Polymer* (in press).
12. Capron, I., Brigand, G. and Muller, G., *Polymer* (submitted).
13. Smith, I. H., Symes, K. C., Lawson, C. L. and Morris, E. R., *Int. J. Biol. Macromol.*, 1981, **3**, 129.
14. Stokke, B. T. and Elgsaeter, A., *Carbohydr. Res.*, 1987, **160**, 13.
15. Miles, M. J., Lee, I. and Atkins, E. D. T., *J. Vac. Sci. Technol.*, 1991, **B9**, 1206.
16. Wilkins, M. J., Davies, M. C., Jackson, D. E., Mitchell, J. R., Roberts, C. J., Stokke, B. T. and Tendler, S. J. B., *Ultramicroscopy*, 1993, **48**, 197.
17. Gunning, A. P., McMaster, T. J. and Morris, V. J., *Carbohydr. Polym.*, 1993, **21**, 47.
18. Kirby, A. R., Gunning, A. P., Morris, V. J. and Ridout, J., *Biophysical J.*, 1995, **68**, 360.
19. Meyer, A., Rouquet, G., Lecourtier, J. and Toulhoat, H., in *Physical Chemistry of Colloids and Interfaces in Oil Production*, eds. H. Toulhoat and J. Lecourtier. Edition technip., Paris, 1992, pp. 275–278.
20. Kirby, A. R., Gunning, A. P. and Morris, V. J., *Carbohydr. Res.*, 1995, **267**, 161.
21. Stokke, B. T., Smidsrod, O. and Elgsaeter, A., *Biopolym.*, 1989, **28**, 617.
22. Ross-Murphy, S. B., Morris, J. and Morris, E. R., *Faraday Symposium Chem. Soc.*, 1983, **18**, 115.
23. Kolodziej, E. J., Paper SPE 16730 presented at the 62nd Annual Technical Conference and Exhibition of the Society of Petroleum Engineers, Dallas, September 1987, pp. 349–364.
24. Moorhouse, R., Walkinshaw, M. D. and Arnott, S., in *Exocellular Microbial Polysaccharides*, eds. P. A. Sandford and A. Laskin. A.C.S. Symp. Series 1977, Vol. 45, Washington, D.C., pp. 81–89.
25. Sho, T., Sato, T. and Norisuye, T., *Biophys. Chem.*, 1986, **25**, 307.
26. Milas, M. and Rinaudo, M., *Carbohydr. Res.*, 1979, **76**, 189.